



POLITECNICO
MILANO 1863

SCUOLA DI INGEGNERIA INDUSTRIALE
E DELL'INFORMAZIONE



Pickering emulsion investigations

APPLIED PHYSICAL CHEMISTRY PROJECT

Author: Elvira Kazimova, Andrea Somma, Giovanni Tomaciello, Sabrina Ulivelli, Giovanni Madella.

Professor: Davide Moscatelli
Academic Year: 2022-23

GROUP29

Abstract

The present work gives an insight on Pickering emulsions, which are a particular type of emulsions that uses solid colloidal particles as stabilizers and have gained rising popularity in the past decades thanks to their ability to prevent the droplets from coalescing and their non-toxic behavior. A collection of existing mathematical models for the investigation of different aspects regarding this matter is reported in this study, these aspects being: the kinetics of formation of the droplets, the droplets stabilization time and the droplets size.

Keywords: Pickering emulsions, kinetics of formation, droplet stabilization time, droplet size.

Contents

Abstract	i
Contents	iii
Introduction	1
1 Kinetics of formation of pickering emulsions	5
1.1 Mathematical model	5
1.2 Experimental evaluation of parameters	8
1.3 Conclusion	9
2 Oil droplet stabilization time in turbulent suspensions	11
2.1 Introduction	11
2.2 Mathematical model	11
2.3 Comparison of model to data	13
2.3.1 Delvigne et al. (1987) data	13
2.3.2 Payne et al.(1989) data	14
2.4 Model application and conclusion	16
3 Prediction of droplet size with oppositely charged particles	19
3.1 Introduction	19
3.2 Modified limited coalescence model	19
3.3 Predictions from the model	21
3.4 Possible causes of deviation	24
3.5 Conclusion	25
4 Langevin dynamics model	27
4.1 Introduction and mathematical model	27
4.2 Simulation details	30
4.3 Results and conclusions	32

Bibliography	35
List of Figures	37
List of Tables	39

Introduction

Emulsions are defined as fine dispersions of minute droplets of a liquid in another immiscible one, which are frequently established either spontaneously or due to mechanical stirring. Emulsions are constituted of continuous and dispersed phases, where the droplet formed in the dispersed phase is, in most cases, hung in the continuous one. Steady emulsions are able to be gained utilizing substances noted as emulsifiers that can diminish the interfacial tension. The said chemical species have amphiphilic properties (both hydrophilic and lipophilic) and they tend to organize at the edges of the present fluids. The formation of a coalescence-resisting protective film and phase separation, that contribute to the emulsion stabilization, are outputs of the adsorption of the additives at the mentioned interface. Traditional emulsion-stabilizers include low molar mass surfactants such as sodium dodecyl sulfate or surface-active polymers.

Emulsions set by solid particles are called Pickering emulsions. Over the last 20 years, Pickering emulsions have been obtaining rising attention and research interest, as the use of traditional surfactants has been impugned owing to environmental, health and cost issues. To stabilize the mixture not ending up in coalescence, only solid particles that accumulate at the interface between two immiscible liquids are suitable for Pickering emulsions.

The great research interest is justified specifically due to the following advantages:

1. solid particles decrease the possibility of coalescence as a "rigid barrier", improving the stability of the emulsions;
2. many solid particles can impart useful characteristics to ready materials, such as conductivity, porosity responsiveness, and so on.
3. Some food-grade solid particulates have less toxicity, resulting in greater safety for consumers.

Many researchers have pointed out that a large amount out of inorganic and organic sediments, including clay, silica, and hydroxyapatite (HAP), can serve as solid surface-active agents. The core factors that influence the stability of emulsions are wettability and particle size. The utilization of dual wettability particles in Pickering emulsions is required to enable stable conditions in water and oil phases. Moreover, another important factor that impacts the longevity

Introduction

of the Pickering emulsions is the size of solid particles. It is extremely significant to have the size of the particles less, at least, 10 times than the droplet size, else, the absorption of the particles at the interface for stabilization is unlikely to occur. In the case of oil-water emulsions solid species are irrevocably adsorbed at the interface, subsequently forming a steric barrier as a result of having suitable wettability and size, preventing aggregation of oil droplets. No less important factor that affects the stability is the shape of particles: they can be spherical, fibrous, polygonal, ellipsoidal, or rod-shaped. As solid components that express high contact angles are able to wet both phases, they are the most fitting to stabilize Pickering emulsions.

Two main mechanisms regulate solid driven emulsions: the first one considers that solid particles are adsorbed at the oil–water interface to constitute a monolayer of particles that can be considered as a rigid film that provides a mechanical barrier to coalescence. The irreversibility of the particle attachment usually results in a more efficient stabilization than the adsorption of surfactants. The contact angle (θ) of the particles with the aqueous phase will lead to O/W emulsion if $\theta < 90^\circ$ (e.g., silica, clay), and to W/O if $\theta > 90^\circ$ (e.g., carbon black) (fig.1). In fact, the particles can stay either in one of the two liquids, in case, they are too hydrophobic or too hydrophilic. The second mechanism is based on particle–particle interactions, leading to the formation of a three-dimensional network of particles in the continuous phase, resulting in an enhanced durability.

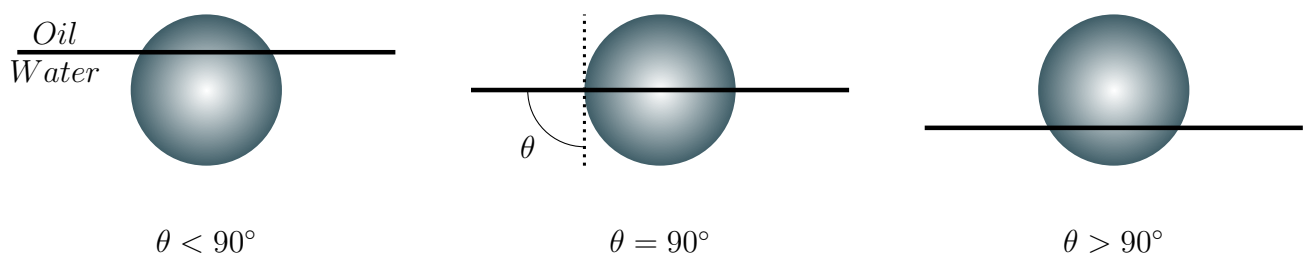


Figure 1: Representation of different contact angles.

| Introduction

Enhanced stability, environmental friendliness and biocompatibility are the most significant pros of Pickering emulsions in comparison to traditional emulsions stabilized by surfactants. Such advantages access their use in a wide range of industries, as food, oil recovery, pharmaceuticals, biomedicine, and cosmetics. In the provided work the usage of Pickering emulsions in the treatment of spilled oils is vindicated, as sometimes the low-concentration pollutants appearing in the form of $0.04\text{--}50 \mu\text{m}$ emulsion droplets are challenging to manage through ordinary methods, for example, centrifugation or gravity separation, which are responsible for severe detriment to the ecological environment and risk human health. Based on this, here the usage of solid particles, as a medium, is considered to induce the Pickering droplets to recover the spilled crude oils (fig.2).



Figure 2: Oil spills in Mexican gulf, Cynthia.

1

Kinetics of formation of pickering emulsions

Reference article: [9].

Reference codes: Emulsification-rate.m, fitting-main.m

1.1. Mathematical model

This study investigates the formation of a pickering emulsion (PE) using water, oil and sand as the solid emulsifier, where water is the continuous phase and oil is the dispersed one, usually, it is indicated as O/W emulsion. The motivation behind choosing this system is to study the potential applicability in marine environment in order to reproduce the concept of PEs in cleaning of oil spills since the implemented solid particles are usually non-toxic as opposed to surfactants. The considered system consists freely dispersed sediments in a continuous liquid phase, where a minor fraction of immiscible pollutant is also present. For the sake of clarity some parameters are defined:

- N_S : Number concentration of solid particles.
- X_{DP} : Volume fraction of dispersed phase.
- N_{PE} : Number concentration of PE droplets.
- V : Average volume per PE droplet.
- n : Average number of solid particle per PE droplet.
- χ : Interaction parameter.
- p : Probability of grouping.

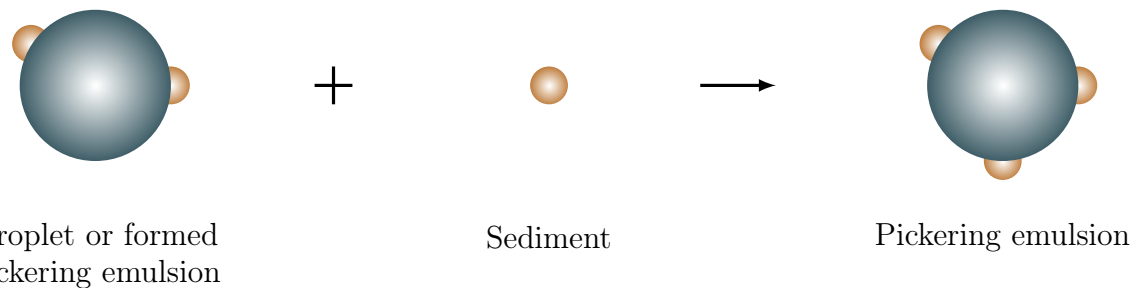
The interaction parameter depends on different factors such as the size of PE droplets, solid particle size, wetting properties at the triple contact line, densities of the phases, stirring rate and the viscosities of the fluids. The probability of grouping represents the collision frequency of

1| Kinetics of formation of pickering emulsions

particles with the available oil droplets. In order to develop a kinetic model some assumptions are made:

1. Diffusion is neglected because the system is vigorously stirred and the sand particles are sufficiently large, so advection is the main transport mechanism.
2. The total surface energy of the system is modest if the contact angle that one of the phases forms with the solid particles is between 0° and 180° .
3. $p = p(N_S, X_{DP})$ Since all the other parameters that may affect this probability are included in χ .
4. The interaction parameter is constant with time.
5. PEs are kinetically "stable" enough to neglect backwards reactions.

Considering a first order kinetic for the following phenomena



and a batch-like model, the mass conservation for PE particles is:

$$\frac{dN_{PE}}{dt} = \chi \cdot p \quad (1.1)$$

Note that no proportionality constant is present because χ already accounts for it. By developing p with the chain rule and introducing some observations based on the conservation of mass it is possible to demonstrate that:

$$\frac{dp}{dt} = - \left(n \frac{\partial p}{\partial N_S} + V \frac{\partial p}{\partial X_{DP}} \right) \cdot \frac{dN_{PE}}{dt} \quad (1.2)$$

Differentiating eq.1.1 once with respect to time and substituting eq.1.2 yields:

$$\frac{d^2N_{PE}}{dt^2} = -\chi \tilde{p} \cdot \frac{dN_{PE}}{dt} \quad (1.3)$$

1| Kinetics of formation of pickering emulsions

where:

$$\tilde{p} = \left(n \frac{\partial p}{\partial N_S} + V \frac{\partial p}{\partial X_{DP}} \right) \quad (1.4)$$

This ODE is analytically solvable with the following conditions:

$$\begin{cases} N_{PE}(t = 0) = 0 \\ N_{PE}(t = \infty) = N_{final} \end{cases} \quad (1.5)$$

So the obtained solution is:

$$N_{PE}(t) = N_{final}(1 - e^{-\chi \tilde{p} \cdot t}) \quad (1.6)$$

In order to find a way to express \tilde{p} eq.1.6 is differentiated with respect to time and for $t = 0$.

$$\tilde{p} = \frac{p(0)}{N_{final}} \quad (1.7)$$

Since χ contains all the proportionality constant, $p(0) := 1$ can be defined and, as a consequence, the solution becomes:

$$N_{PE}(t) = N_{final}(1 - e^{-\frac{\chi \cdot t}{N_{final}}}) \quad (1.8)$$

Plotting this expression as a function of time, the following graph is obtained:

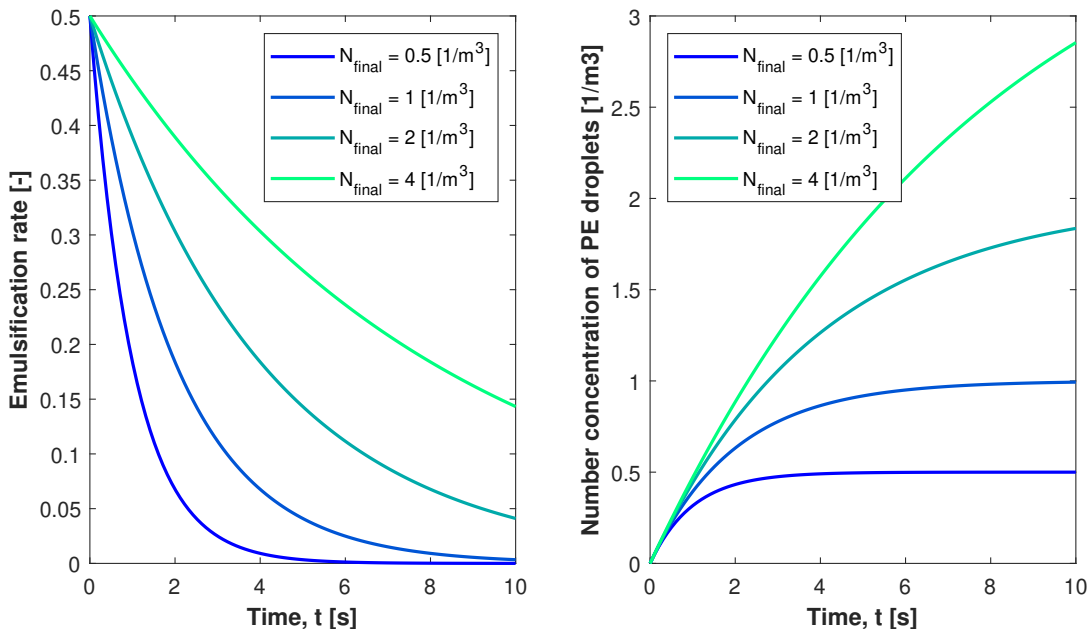


Figure 1.1: Emulsification rate and number concentration of PE droplets as a function of time, with constant $\chi = 0.5$.

1| Kinetics of formation of pickering emulsions

1.2. Experimental evaluation of parameters

Even if the result is straightforward it is necessary to evaluate the parameters N_{final} and χ ; in order to achieve this the parameter $k := \frac{\chi}{N_{final}}$ is defined and can be found through experimental data. Since the goal is to emulsify the entirety of a petroleum system, the experiment is designed assuming that $\frac{X_{DP}(0)}{V} < \frac{C_{DP}(0)}{n}$ this implies that $N_{final} = \frac{X_{DP}(0)}{V}$.

For simplicity, eq.1.8 is manipulated to get the following expression:

$$\frac{N_{PE}}{N_{final}} = 1 - e^{-k \cdot t} \quad (1.9)$$

where $\frac{N_{PE}}{N_{final}}$ is equal to the fraction of emulsified petroleum volume estimated using frame-by-frame software. The experimental system consists in a dish containing sea water, sand and heavy fraction of crude oil. The system is stirred manually and the experiment is performed thrice to ensure repeatability.

With the experimental data of $\frac{N_{PE}}{N_{final}}$ and t is possible to fit the model through the k parameter. This has been done with Matlab[5] using *lsqnonlin* function, that solves nonlinear least-squares curve fitting problems of the form:

$$\min_x \|f(x)\|_2^2 = \min_x (f_1(x)^2 + f_2(x)^2 + \dots + f_n(x)^2),$$

it starts from a first guess value x_0 and follow the gradient up to reaching the requested tolerance. One of the drawbacks is the possibility to find a local minimum without converging in an absolute one. Fitting the data reported in tab.1.1 the resulting value of the k is 0.21.

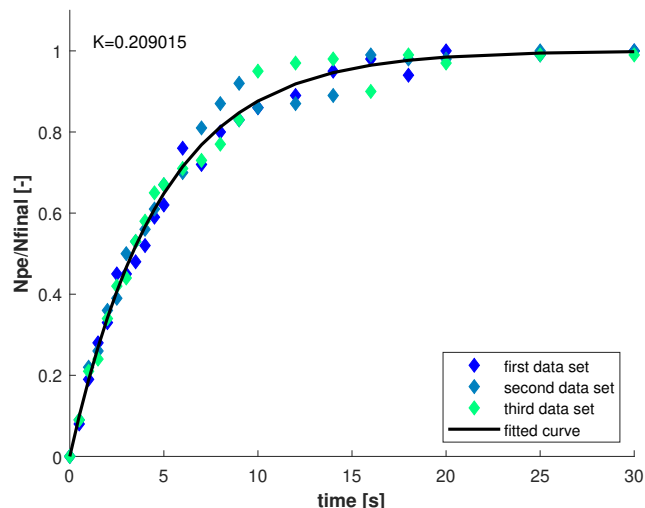


Figure 1.2: Data fitting of the k parameter.

1| Kinetics of formation of pickering emulsions

Data sets used for the fitting are presented below:

t [s]	$\frac{N_{PE}}{N_{final}}$ [-]	$\frac{N_{PE}}{N_{final}}$ [-]	$\frac{N_{PE}}{N_{final}}$ [-]	t [s]	$\frac{N_{PE}}{N_{final}}$ [-]	$\frac{N_{PE}}{N_{final}}$ [-]	$\frac{N_{PE}}{N_{final}}$ [-]
0	0	0	0	7	0.7200	0.8100	0.7300
0.5	0.0800	0.0900	0.0900	8	0.8000	0.8700	0.7700
1	0.1900	0.2200	0.2100	9	0.8300	0.9200	0.8300
1.5	0.2800	0.2600	0.2400	10	0.8600	0.8600	0.9500
2	0.3300	0.3600	0.3400	12	0.8900	0.8700	0.9700
2.5	0.4500	0.3900	0.4200	14	0.9500	0.8900	0.9800
3	0.4500	0.500	0.4400	16	0.9800	0.9900	0.9000
3.5	0.4800	0.5300	0.5300	18	0.9400	0.9800	0.9900
4	0.5200	0.5600	0.5800	20	1	0.9800	0.9700
4.5	0.5900	0.6100	0.6500	25	0.9900	1	0.9900
5	0.6200	0.6700	0.6700	30	1	1	0.9900
6	0.7600	0.7000	0.7100				

Table 1.1: Three different data sets for $\frac{N_{PE}}{N_{final}}$ with respect to time

1.3. Conclusion

As can be seen, the theoretical model fits very well the experimental data, even if the proposed expression is practically a function of a single parameter. This is the proof that the proposed framework may be used to predict the evolution of the presented system, and that sand could be used as an effective emulsifier for oil-spills in seawater (fig.1.3a and 1.3b). To achieve its applicability, it is necessary to deepen the dependance of χ upon the system parameters, and to better understand how combine PEs with digesting bacterias, in order to reach the oil-spill cleaning, where the oil trapped in the emulsion is degraded by bacteria and transformed into non-toxic chemicals.

1| Kinetics of formation of pickering emulsions

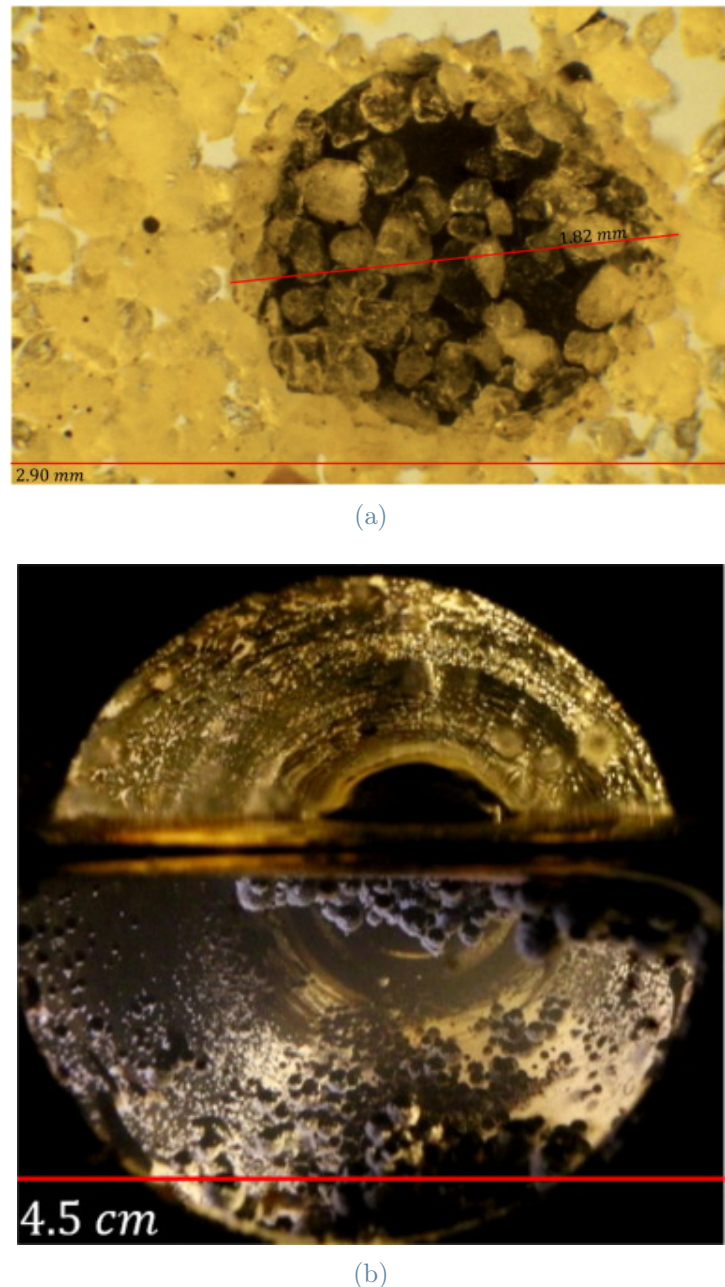


Figure 1.3: Formed Pickering emulsions in an oil-water system with sand as solid emulsifier.

2 | Oil droplet stabilization time in turbulent suspensions

Reference article: [3]

Reference codes: OMA-time-stab.m, alpha-min.m, tc-ex.m.

2.1. Introduction

In this section, the study, coming from a further scientific paper of the Department of Oceanography, Dalhousie University, Halifax, NS, Canada and the Marine Environmental Sciences Division, Bedford Institute of Oceanography, Dartmouth, NS, Canada, has been introduced in order to strongly confirm the proposed model with more experimental data and to deepen the phenomena in more aspects. In particular, the authors, starting from the observation of the naturally remotion of oil from shorelines, hypothesize that formation of oil-mineral aggregates (OMAs) in sea water is the reason for this phenomenon, and they present a kinetic model that equals the one that has been investigated previously. The interesting and unreleased thing about this research work is that they focus on the time in which oil in water emulsions (or aggregates) stabilize, and its dependence on the oil droplet and sediment particle size.

2.2. Mathematical model

The mentioned system is formed by droplets of oil and sediment particles suspended in a turbulent continuous phase (sea water). Many interactions can happen: sediment particles collision with each other, oil droplets coalescence and aggregation of sediment particles with oil droplets. This requires a very complex model that can be solved only with an elaborated computational task. However, a simplified model, that focuses on the only dominant interactions, can be adopted. The said model is based on various assumptions:

1. The suspension of oil and sediment is well mixed in three dimensions.
2. Particle collisions occur solely due to motion.

2| Oil droplet stabilization time in turbulent suspensions

3. The size of sediment particles is much less than the size of oil droplets ($D_s \ll D_o$).
4. Sediment-sediment and oil-oil collisions do not result in coalescence.
5. Sediment particles and oil droplets can be characterized by a mean sediment diameter and a mean droplet diameter.
6. Interaction between sediment and oil is irreversible.

According to the assumptions above, the rate of change of sediments **number concentration**, because of collisions with oil, can be written as a power law[8] , whose kinetic coefficient depends on the size of sediment particles and oil droplets (D_s, D_o), the physical properties of turbulent suspension in which they are dispersed, and the oil-sediment coalescence efficiency (α_{os}):

$$\frac{dN_s}{dt} = -0.16\alpha_{os}(D_s + D_o)^3 \left(\frac{\varepsilon}{\nu}\right)^{\frac{1}{2}} N_s N_o \quad (2.1)$$

In which N_s is the sediment number concentration, N_o is the oil droplet number concentration, ε is the turbulent-kinetic-energy dissipation rate and ν is the kinematic viscosity of water. Integrating this expression from 0 to a generic time t , the number of sediment particles per unit of volume removed from suspension (ΔN_s) in time t is:

$$\Delta N_s = N_s(0) [1 - \exp(-\beta t)] \quad (2.2)$$

$$\beta = 0.16\alpha_{os}(D_s + D_o)^3 \left(\frac{\varepsilon}{\nu}\right)^{\frac{1}{2}} N_o \quad (2.3)$$

This model allows to calculate the time required to stabilize the oil-sediment aggregate suspended in aqueous phase. This condition is reached when sediment cover all droplets with an ordered hexagonal close-packed arrangement, according to geometrical and physical considerations[10]. The number concentration of sediment required is:

$$N_{sc} = \frac{2\pi}{\sqrt{3}} \left(\frac{D_o}{D_s}\right)^2 N_o \quad (2.4)$$

Substituting this value in eq.2.2 and solving for time, the critical one can be derived:

$$t_c = -\frac{\ln \left(1 - \frac{2\pi}{\sqrt{3}} \left(\frac{D_o}{D_s}\right)^2 \frac{N_o}{N_s(0)}\right)}{\beta} \quad (2.5)$$

2.3. Comparison of model to data

2.3.1. Delvigne et al. (1987) data

In order to verify the model, many experiments have been done. In particular, variables in Delvigne et al.[2] experiment can be used to calculate the minimum value of coalescence efficiency. The range of this variable must be relatively low in the experimental conditions, so if the requirement is respected the model can not be rejected.

In Delevigne et al. experiment sediment and oil were put into a water phase that is perturbed by two agitation energies that are characterized by two different values of ε . Three kind of oil and two types of sediment (kaolinite and silt) in different initial concentration were used. For all possible combinations the experiment calculates the equilibrium time of the system in which the minimum value of α is reached. However, in the experimental condition the equilibrium state does **not correspond to the stabilization of aggregates**. Rather it equals to the time required to form negatively buoyant clusters. This state is reached when the number of sediments removed from the suspension is:

$$\Delta N_s = N_o \left(\frac{D_o}{D_s} \right)^3 \frac{\rho - \rho_o}{\rho_s - \rho} \quad (2.6)$$

Combining the eqs.2.2 and 2.6, the values of the minimum coalescence efficiency for every combination are calculated as written here:

$$\alpha_{min} = - \frac{\ln \left[1 - \frac{N_o}{N_s(0)} \left(\frac{D_o}{D_s} \right)^3 \frac{\rho - \rho_o}{\rho_s - \rho} \right]}{0.16 t_e (D_s + D_o)^3 \left(\frac{\varepsilon}{\nu} \right)^{\frac{1}{2}} N_o} \quad (2.7)$$

where:

$$N_o = \frac{C_o}{\frac{4}{3}\pi \left(\frac{D_o}{2} \right)^3 \rho_o} \quad (2.8)$$

$$N_s = \frac{C_s}{\frac{4}{3}\pi \left(\frac{D_s}{2} \right)^3 \rho_s} \quad (2.9)$$

$$D_o = 0.005 \nu_o^{0.34} \varepsilon^{-0.5} \quad (2.10)$$

experimental equation

2| Oil droplet stabilization time in turbulent suspensions

Obtaining the following results:

$C_s [kgm^{-3}]$	$C_o [kgm^{-3}]$	$\varepsilon [m^2s^{-3}]$	$\nu_o [m^2s^{-1}]$	$\rho_o [kgm^{-3}]$	$D_o [m]$	$t_e [s]$	$\alpha_{min} [-]$
0.06	0.1	3.43	9.2e-05	900	1.1e-4	1200	0.006
0.02	0.035	3.43	9.2e-05	900	1.1e-4	1200	0.017
0.006	0.1	3.43	9.2e-05	900	1.1e-4	3600	0.019
0.06	0.1	3.43	1.22e-04	902	1.3e-4	1200	0.006
0.06	0.1	0.43	1.22e-04	902	3.6e-4	1200	0.017
0.06	0.1	0.43	8e-06	808	1.4e-4	1200	0.041
0.06	0.1	3.43	8e-06	808	5e-5	1200	0.013

Table 2.1: Experimental data of Delvigne et al.(1987) and calculated values of α_{min}

As shown in tab.2.1, the obtained values of α_{min} are in the range 0.006-0.041. This low range of coalescence efficiency is consistent with the condition in which the experiment has been conducted. In fact, because of electrochemical and hydrodynamic forces, there are series of constraints that inhibit the contact between particles, and consequently the rate of the emulsion formation. So, this results are accurate and, moreover, they can not refuse the proposed model.

2.3.2. Payne et al.(1989) data

To validate the kinetic law, other experimental data can be used. For example, the Payne et al.(1989)[7] series of experiments gives a different view of the phenomenon, but achieving the same results. In fact, in this case, the study focuses on the rate of decay of free oil droplets instead of sediment particles. Assuming that, **each loss of sediments particle results in the loss of one oil droplet**, one can achieve the same expression above, but in terms of oil droplet mass concentration:

$$\frac{dC_o}{dt} = -kC_o \quad (2.11)$$

where:

$$k = 0.16\alpha_{os}(D_s + D_o)^3 \left(\frac{\varepsilon}{\nu}\right)^{\frac{1}{2}} N_s \quad (2.12)$$

The aim of the experiment is to estimate the values of the coalescence efficiency again and to compare it with the previous values already discussed. However, in this case, the experiment uses a different coefficient, called A and defined as:

$$A = \frac{k}{0.16\left(\frac{\varepsilon}{\nu}\right)^{\frac{1}{2}} C_s} \quad (2.13)$$

2| Oil droplet stabilization time in turbulent suspensions

Combining the eqs.2.12 and 2.13 the following expression can be obtained:

$$A = \alpha_{os} \frac{N_s}{C_s} (D_s + D_o)^3 = \alpha_{os} A_{theory} \quad (2.14)$$

$$D_s = \left(\frac{6Cs}{\rho_s \pi N_s} \right)^{\frac{1}{3}} \quad (2.15)$$

where A can be estimated experimentally, and A_{theory} can be calculated analytically. Therefore, the coalescence efficiency α_{os} represents the slope of the line formed by A and A_{theory} , and it can be calculated by a linear regression. Applying this method, the results, that have been obtained, are:

$N_s/C_s [kg^{-1}]$	$\rho_s [kgm^{-3}]$	$D_s [\mu m]$	$D_o [\mu m]$	$A_{obs} [m^3 kg^{-1}]$	$A_{theory} [m^3 kg^{-1}]$	$\alpha_{os} [-]$
178e12	2760	1.6	6	12.2e-5	0.077	0.0016
56e12	2640	2.3	6	2.5e-5	0.033	0.0008
11e12	2770	4.0	6	1.6e-5	0.011	0.0015
56e12	2550	2.4	6	7.0e-5	0.033	0.0021
56e12	2510	2.4	6	6.8e-5	0.033	0.0021
42e12	2510	2.6	6	3.4e-5	0.027	0.0012
16e12	2700	3.5	6	2.2e-5	0.014	0.0016

Table 2.2: Experimental data of Payne et al.(1989) and obtained values of α_{os}

Specifically, gained values for α_{os} are, averagely, an order of magnitude less than the ones presented in the previous tab.2.1, since the one-to-one particle-sediment collision assumption has been made.

2| Oil droplet stabilization time in turbulent suspensions

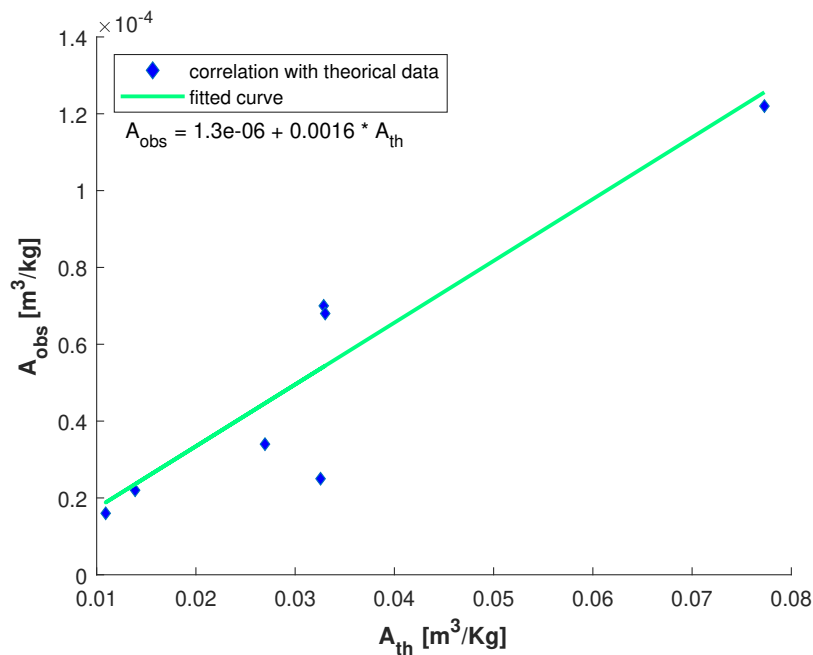


Figure 2.1: A_{obs} vs A_{theory} from Payne et al. (1989)

In the developed equation for A (eq.2.14) the value of the expression at the initial point should be equal to zero, in contrast to what is shown in the linear regression, anyways this does not affect the accuracy of the model, since the value of the y-intercept is negligible ($1.3e - 6$).

2.4. Model application and conclusion

The kinetic model can be used to calculate the stabilization time of emulsions of oil droplets in turbulent suspensions. As discussed previously, this value depends on different parameters according to the physical and chemical condition of the system. In particular, there is a strong dependence on the size of oil and sediment particles, on the turbulence of the continuous phase, and on the concentration of oil and sediment. To include this large variability, it's appropriate to consider three values for each variable and to derive the stabilization time for **every possible combination**. The chosen variable ranges are:

2| Oil droplet stabilization time in turbulent suspensions

Variable	Values
Sediment diameter, $D_s(\mu m)$	1,2,4
Droplet diameter, $D_o(\mu m)$	6,30,150
Sediment mass concentration, $C_s(kgm^{-3})$	0.02,0.2,2.0
Oil mass concentration, $C_o(kgm^{-3})$	0.01,0.03,0.1
Turbulent kinetic energy dissipation rate, $\varepsilon(m^2 s^{-3})$	$10^{-3}, 10^{-1}, 10$
Coalescence efficiency, α_{os}	0.001,0.005,0.025

Table 2.3: Variables range to calculate OMA stabilization time

where values of D_s and oil concentration has been taken from the Payne et al. (1989), the range of D_o and ε from Delvigne et al. (1987) , the concentration of sediment particles from the typical concentration in coastal environments, and the coalescence efficiency values from the experimental data that have been discussed previously (tab.2.1 and 2.2).

So, using the eq.2.5 for all possible combinations, ones can calculate the stabilization time of oil droplets. As expected, the results are very scattered, with values that range from seconds to hours. This state leads that the most useful analysis is to bin the time in different domains, and to evaluate the distribution of the critical times in the identified ranges. The different time scales correspond to different physical processes that characterize the system. They move from turbulent phase, where OMAs stabilize in less than one second, to physical conditions where OMAs can not stabilize or, in other words, OMAs require infinity time for stabilization.

2| Oil droplet stabilization time in turbulent suspensions

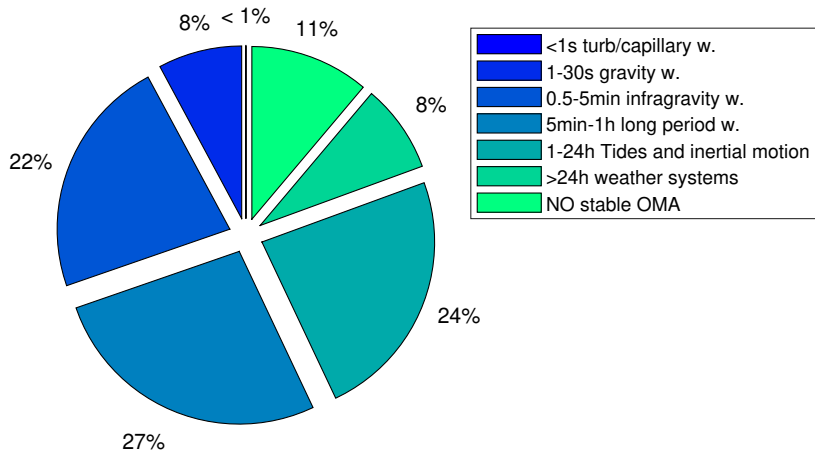


Figure 2.2: Distribution of OMA stabilization time lengths in time scale ranges

As shown, OMA stabilization time lengths that span from minutes to a day are the most common (over a half of the time belongs in this range). About one fifth of the time lengths is shorter than 30 seconds, and one tenth is longer than a day. The results above demonstrate that the sediment concentration is the parameter that produces the main effect in the stabilization time. In fact, the shorter time lengths occur when the sediment concentration is high and droplets are large, and, in this case, OMAs stabilize instantaneously. However, this conditions are far from the ones that are in nature. Under typical natural sediment concentrations, stable OMAs form in minutes to hours.

3

Prediction of droplet size with oppositely charged particles

Reference article: [6]

Reference codes: size-droplet.m

3.1. Introduction

The model proposed in this section has been developed to estimate the droplet size in pickering emulsions stabilized by oppositely charged particles (OCPs), it is based on the hypotheses that OCPs form stable clusters thanks to the strong electrostatic attractions between them, and that the formed clusters act as stabilizers. This is a model with two parameters, being:

- k : ratio of effective charge of OCPs.
- X : number of particles contained in the formed cluster.

The model predicts that the droplet size varies non-monotonically with the number ratio of oppositely charged colloids, and it shows a minimum. The theoretical estimation is also in agreement with the results of the corresponding experimental study.

3.2. Modified limited coalescence model

The studied model is only applicable after making some assumptions:

1. Oppositely charged particles have the same size.
2. Highly charged particles cannot stabilize emulsions if they are implemented alone.
3. The OCPs combine by forming aggregates when they are mixed in the water phase and it is possible that they combine in a ratio that neutralizes the charges. The factor k describes how the OCPs combine: if $k = 1$ there is the same amount of positive and negative particles, if $k < 1$ the number of positive particles is lower, and if $k > 1$ the number of positive charges is higher.

3| Prediction of droplet size with oppositely charged particles

4. When OCPs are mixed it happens that some particles will aggregate while others will remain in the water phase, this depends on the concentrations of both solid species.
5. Only the particles that form the aggregates contribute to the stabilization.
6. Since the aggregates are the only species stabilizing the emulsion, the size, shape and concentration of the final droplets is only influenced by them.
7. The aggregates are spherical and form a monolayer at the interface.

Considering N_T the total concentration of particles in water, N_P and N_N the number concentration of positive and negative particles, if all particles can be found in the water phase, one can express N_T as:

$$N_T = N_P + N_N \quad (3.1)$$

And a new parameter, defined "composition", can be introduced:

$$\Phi_P = \frac{N_P}{N_P + N_N} \quad (3.2)$$

The "critical composition" (Φ_P^*) occurs when N_N becomes limiting to the system, which means that all the particles participate to the stabilization and there are no particles which remain in the water phase. For the sake of the following discussion, the variable N_{eff} can be defined, it acts for the particles that effectively combine to form neutral aggregates.

To determine the droplet diameter, three different cases must be studied:

1. If $\Phi_P < \Phi_P^*$ eq.3.3 can be written:

$$N_P = \Phi_P N_T \quad (3.3)$$

Furthermore, the concentration of negative particles N_N^* that combine with N_P positive particles per unit of volume is:

$$N_N^* = k N_P \quad (3.4)$$

and the number of effective particles can be expressed as:

$$N_{eff} = N_P + N_N^* = (1 + k) \Phi_P N_T \quad (3.5)$$

2. If $\Phi_P = \Phi_P^*$ then $N_{eff} = N_T$, one can define the critical composition as:

$$\Phi_P^* = \frac{1}{1 + k} \quad (3.6)$$

3| Prediction of droplet size with oppositely charged particles

3. If $\Phi_P > \Phi_p^*$ the negative particles are limiting, the number of effective particles is:

$$N_{eff} = (1/1 + k)(1 - \Phi_P)N_T \quad (3.7)$$

Once the number of effective particles has been defined, the concentration of the aggregates can be calculated as:

$$N_X^{agg} = \frac{N_{eff}}{X} \quad (3.8)$$

If it is assumed that all the aggregates are spherical and of the same size, their radius can be written as follows:

$$R_X^{agg} = a \sqrt[3]{X(1 + \rho)} \quad (3.9)$$

where a is the radius of the particles and ρ is the internal voidage of the aggregates. The cross-sectional area of the aggregates, which is $A_X^{agg} = \pi(R_X^{agg})^2$, is given by:

$$A_X^{agg} = \pi a^2 \sqrt[3]{(X(1 + \rho))^2} \quad (3.10)$$

Finally, for the described system, the equations for the droplets diameter in the 3 cases can be derived:

$$D = \begin{cases} \frac{6s}{N_T \pi a^2 (1+k) \Phi_p X^{-1/3} (1+\rho)^{2/3}}, & \text{if } \Phi_p < \Phi_p^* \\ \frac{6s}{N_T \pi a^2 X^{-1/3} (1+\rho)^{2/3}}, & \text{if } \Phi_p = \Phi_p^* \\ \frac{6s}{N_T \pi a^2 (1+\frac{1}{k}(1+\Phi_p)) X^{-1/3} (1+\rho)^{2/3}}, & \text{if } \Phi_p > \Phi_p^* \end{cases} \quad (3.11)$$

where s is the droplet surface coverage, considered equal to 0.9069 for a sediment monolayer.

3.3. Predictions from the model

As has been described above, the modified limited coalescence model introduces two new parameters which influence the droplet diameter dimension, when working with electrically charged particles. These two parameters are k and Φ_P .

3| Prediction of droplet size with oppositely charged particles

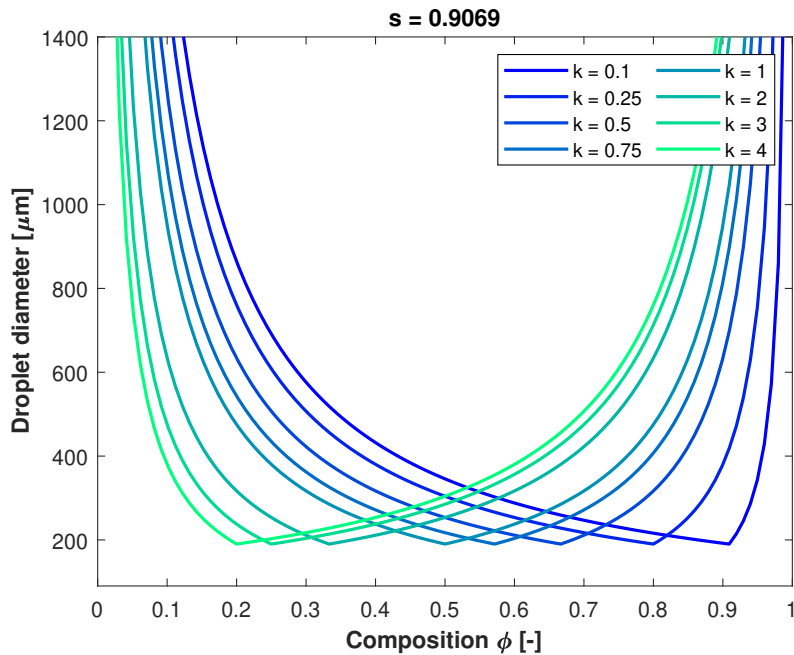


Figure 3.1: Variation of droplet diameter with composition.

The curves in fig.3.1 show how the droplet diameter changes with the composition of particles Φ_P , for a given value of k . Two observations can be made from the obtained trends:

1. There is a **non-monotonic** variation of the diameter with increasing composition. The minimum droplet size occurs when the OCPs combine to form the maximum number of aggregates, hence when the concentration of effective particles is the maximum.
2. k is responsible for a shift in the composition at which the minimum diameter occurs, either to the left or to the right of the graph. This happens because when the charge on the surface of one of the two types of particles is higher, for example, if positive particles are more charged, in order to form stable aggregates, each of these particles will have to combine with more than one of the negative ones. In fact, if positive particles are more charged then $k > 1$, and vice versa, from the figure it can be observed that the composition at which the minimum droplet size occurs is $\Phi_P = 0.5$ when $k = 1$, while if $k > 1$ the composition shifts to the left, and if $k < 1$ it shifts to the right.

3| Prediction of droplet size with oppositely charged particles

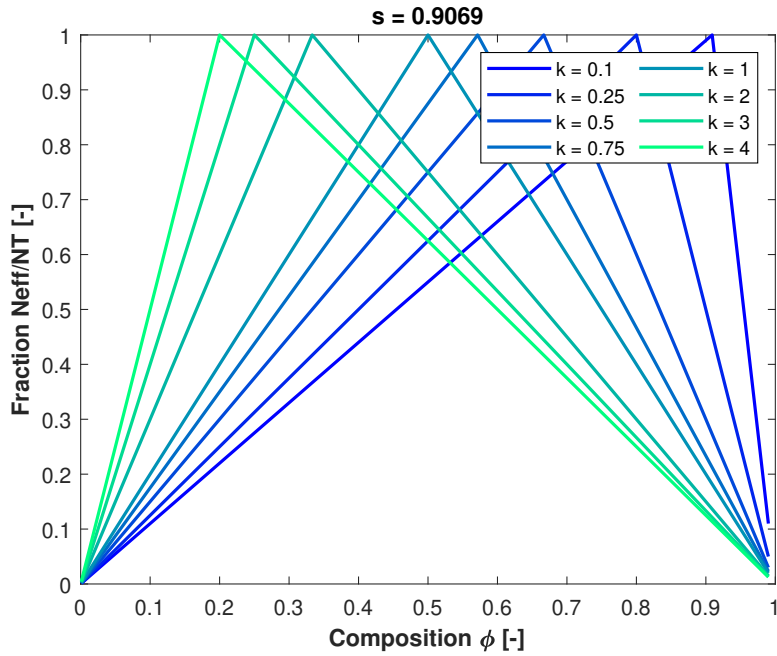


Figure 3.2: Variation of $\frac{N_{eff}}{N_T}$ with composition.

Fig.3.2 shows how the fraction $\frac{N_{eff}}{N_T}$ varies with composition for a given value of k , and the corresponding diameters are those presented in fig.3.1. It must be noted that, the obtained curves follow a linear trend because of the assumption that k is constant. In real systems it can occur that also k is a function of the composition, and this would be responsible for a nonlinear evolution of $\frac{N_{eff}}{N_T}$, which would influence the droplet diameter as well. When the composition is equal to 0 or 1, $\frac{N_{eff}}{N_T}$ is 0. This is because in such conditions there are only pure negative or pure positive particles that are ineffective on their own, so the diameter of the droplets will be infinite and there will be no emulsion formation. Starting from 0, as the composition increases there is an increase in $\frac{N_{eff}}{N_T}$, until the value of 1 is reached, this value corresponds to the composition at which particles combine to a maximum extent, and at which droplets with the minimum possible diameter are obtained. Anyways, k would influence $\frac{N_{eff}}{N_T}$ curve in the same way as the analyzed side.

3| Prediction of droplet size with oppositely charged particles

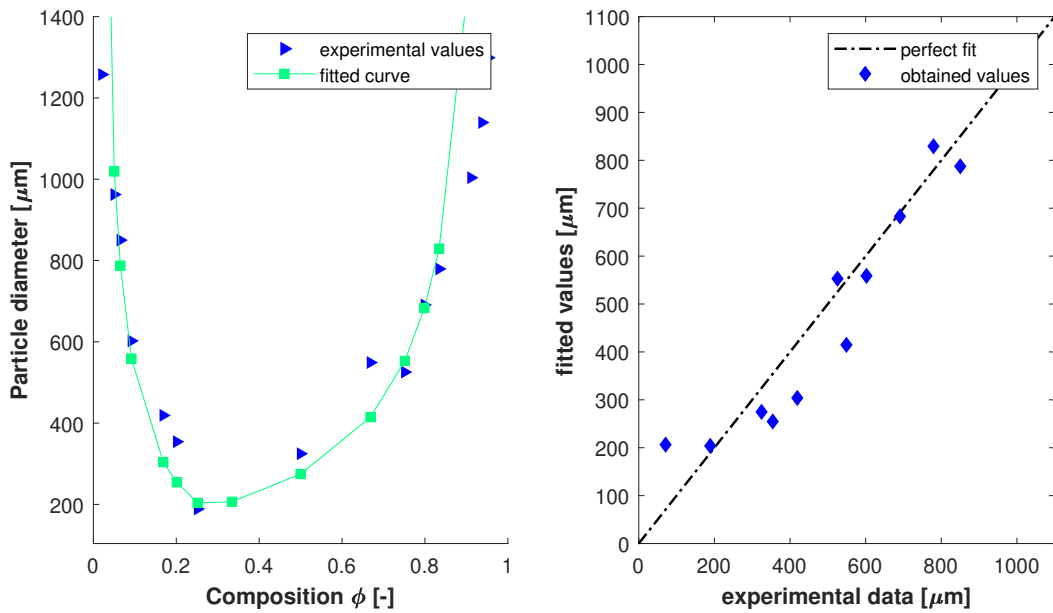


Figure 3.3: Comparison between model and experimental data.

Fig.3.3 is a comparison between the experimental data and the values predicted from the model, it can be observed that the results are coherent, and the model is perfectly acceptable under the previously stated assumptions.

3.4. Possible causes of deviation

It is common to observe deviations from the modified limited coalescence model due to the fact that it is based on simplifying assumptions, that are not always a good approximation of reality. Three of the possible causes are:

- Size and shape of the aggregates:** one of the hypotheses of the model is that all the aggregates are spherical and of fixed size, but in a real system there will most certainly be a distribution of aggregate sizes and shapes. Factors like size, shape, orientation and possible rearrangements of these aggregates at the droplet surface can lead to significant errors between the predicted and observed droplet sizes.
- Concentration of aggregates:** it was assumed that the number of effective particles, and so the concentration of clusters, are simply a direct function of the particle composition of the system (Φ_P). This is true, but some considerations must be added because when the concentration of one of the two types of particle is too high, usually when $\Phi_P < 0.2$ or $\Phi_P > 0.8$, it is possible that not all the sediments and oil combine to generate neutral aggregates, and they are effective in the stabilization. In such cases, it can

3| Prediction of droplet size with oppositely charged particles

occur that the particles combine to form small charged aggregates instead of the neutral ones, influencing the droplet size.

3. **Surface coverage:** the modified limited coalescence model works under the hypothesis that spherical aggregates form a monolayer at the interface, in this case one can assume a surface coverage parameter $s = 0.9069$, and this value, which works for hexagonal packing of spherical particles in 2D, has been used to estimate the trends reported in fig.3.1 and 3.2. It is possible though, that there is the formation of multilayers which causes the observed droplet size to be larger than the predicted one. The curves are reported below in the case of the formation of a double layer of aggregates at the interface, where $s = 1.8138$. It can be noted that, the effect of the surface coverage becomes more relevant when the particles concentrations are high (fig.3.4).

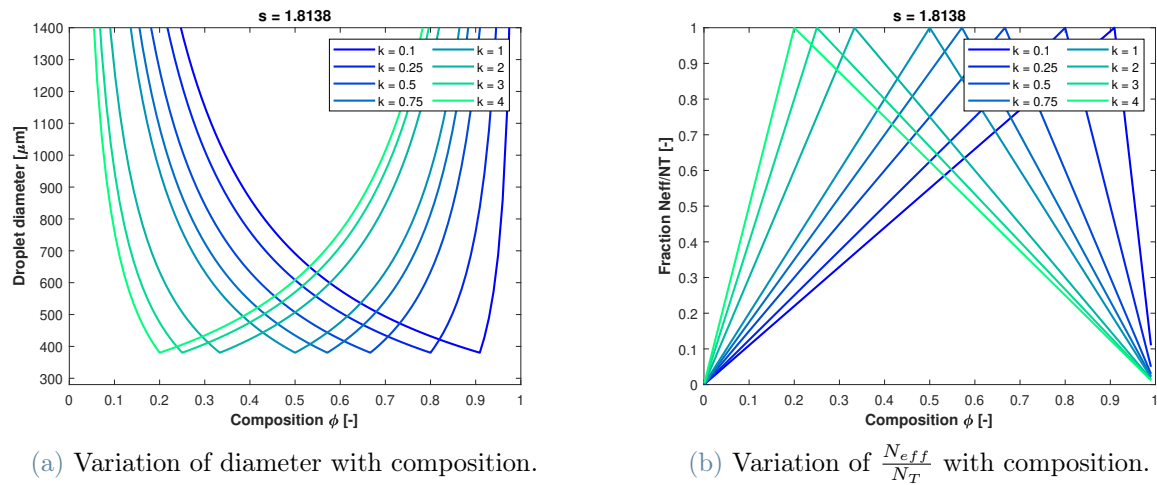


Figure 3.4: Effect of s on emulsion parameters.

3.5. Conclusion

The developed model shows the effect of certain parameters, such as: total particle concentration, composition, and charge ratio on the size of the emulsion drops, when working with OCPs. Factors like particle concentration, energy input, duration of agitation are known to influence the droplet size in pickering emulsions, with the modified limited coalescence model. Two new levers can be introduced to control the droplet diameter: the **charge of the particles**, expressed via the parameter k , and the **composition of the mixture** (Φ_P). It has been seen that, it is possible to work simultaneously on the two variables to obtain the desired droplet size, and this approach is particularly useful when one wants to tune the droplet size while keeping the particle concentration fixed, this is not possible when working with just one type of particles. By the comparison between the model and the experimental data, it has been

3| Prediction of droplet size with oppositely charged particles

shown that this model is able to capture the physics of the process both qualitatively and, to a very good extent, quantitatively.

4 | Langevin dynamics model

Reference articles: [1, 4]

Reference codes: langevin-random.m, postprocessing.py

4.1. Introduction and mathematical model

In this section O/W silica/magnetite Pickering emulsions has been investigated through Langevin dynamics methods, this approach is much different than the ones presented up to now in this work, since the point of view is the molecular one and not the continuous macro-scale. Specifically, Langevin dynamic is used to describe acceleration of a particle in a fluid, as for the purpose of this topic solid particles and oil droplets have been discretized as spheres of various radii, that interact with continuous phase (water) through the drag coefficient. The aforementioned particles also interact with each other due to Vander-Waals forces and cohesion ones in the case of droplet-sediment contact; furthermore, to reproduce the Brownian motion a random component is added, based on the temperature and the particle mass, as in the Boltzmann distribution. To describe what has been depicted above, some correlations have to be introduced in order to analyze the problem in a mathematical way and to implement the whole phenomenon in a code, discretizing in time and space. In particular, a Langevin impulse integrator and a modified rattle algorithm have been coupled, according to the first one the principal equations to solve the system are:

1.

$$v_{t+1\frac{1}{2}\Delta t} = v_t + \frac{F_t}{2m} \Delta t \quad (4.1)$$

Where v is the particle velocity given a certain direction at time step $t + \frac{1}{2}\Delta t$ (a halved time step is chosen for calculating particles velocities in order to increase the stability of the solver), F is the force applied to the said particle at time t and m is the mass of the particle, gravity is not taken into account in this simulation given the dimensions of the particles (fig.4.2b).

4| Langevin dynamics model

2.

$$x_{t+\Delta t} = x_t + \frac{m}{\gamma} (1 - e^{-\frac{\gamma}{m} \Delta t}) v_{t+\frac{1}{2}\Delta t} + \frac{1}{\gamma} \sqrt{2kT\gamma} R_{2,t+\Delta t} \quad (4.2)$$

Where γ is the friction coefficient in water, k is the Boltzman constant, T is the system temperature, and R_2 is a random factor.

3.

$$v_{t+\Delta t} = v_{t+\frac{1}{2}\Delta t} e^{-\frac{\gamma}{m} \Delta t} + \frac{1}{m} \sqrt{2kT\gamma} R_{1,t+\Delta t} + \frac{F_t}{2m} \Delta t \quad (4.3)$$

Where R_1 is an additional random factor, and F_t is the resultant of attraction and repulsion forces acting on the particle.

For the calculation of attraction forces between two particles the following equation is used:

$$F_{at} = -\frac{32}{3} A \frac{r_1^3 r_2^3 (H + r_1 + r_2)}{H^2 (H + 2r_1)^2 (H + 2r_2)^2 (H + 2(r_1 + r_2))^2} \quad (4.4)$$

where A is the Hamaker constant, H is the separation distance between the two surfaces and r is the radius. For the repulsion forces:

$$F_{rep} = \pi \varepsilon \varepsilon_0 \frac{r_1 r_2}{r_1 + r_2} \kappa \left((\zeta_1 - \zeta_2)^2 \frac{e^{-\kappa H}}{e^{-\kappa H} + 1} + (\zeta_1 + \zeta_2)^2 \frac{e^{-\kappa H}}{e^{-\kappa H} + 1} \right) \quad (4.5)$$

where ζ are particles ζ -potentials, κ is the inverse Debye length, ε_0 is the dielectric constant, and ε is the permittivity of the medium, in this case, water. The Brownian motion was modeled as a random force applied at each time-step, the said random components are evaluated as follows:

$$R_{1,t+\Delta t} = \sqrt{\tau_2} \xi_{1,t+\Delta t} \quad (4.6)$$

$$R_{2,t+\Delta t} = \frac{\tau_1 - \tau_2}{\sqrt{\tau_2}} \xi_{1,t+\Delta t} + \sqrt{\Delta t - \frac{\tau_1^2}{\tau_2}} \xi_{2,t+\Delta t} \quad (4.7)$$

$$\tau_1 = \frac{m}{\gamma} (1 - e^{-\frac{\gamma}{m} \Delta t}) \quad (4.8)$$

$$\tau_2 = \frac{m}{2\gamma} (1 - e^{-\frac{\gamma}{m} \Delta t}) \quad (4.9)$$

where ξ are random values obeying a standard normal distribution.

The system of equations written up to now is not solvable "as it is", but it needs some intermediate steps to increase convergence and stability, to do so an **constrained adapted Rattle algorithm** has been implemented. A summarized version is proposed here:

4| Langevin dynamics model

→ Step 1: Calculate half velocities values for all particles with no bonds taken into account:

$$v_{i,n+\frac{1}{2}} = v_{i,n} + \frac{1}{2}a_{i,n}\Delta t \quad (4.10)$$

where a is the acceleration of the particle at time n , and $\frac{1}{2}$ represents the halved time-step.

→ Step 2: Execute the correction on the evaluated velocities of all collided or near to collision particles in pairs (i,j indexes):

⇒ Step 2.1: calculate desired distance $d_{i,j}$:

$$d_{i,j} = r_i + r_j \quad (4.11)$$

⇒ Step 2.2: calculate the relative shift due to the new velocities applied:

$$s_n = (x_{i,n} + \Delta x'_{i,n}) - (x_{j,n} + \Delta x'_{j,n}) \quad (4.12)$$

⇒ Step 2.3: if $|s_n^2 - d_{i,j}^2| < \delta_x$ then go to Step 2.5, otherwise evaluate the correction coefficient:

$$\beta_n = \frac{s_n^2 - d_{i,j}^2}{2s_n(x_{i,n} - x_{j,n})\lambda} \quad (4.13)$$

$$\lambda = \frac{1 - e^{-\frac{\theta_i}{m_i}\Delta t}}{\theta_i} + \frac{1 - e^{-\frac{\theta_j}{m_j}\Delta t}}{\theta_j} \quad (4.14)$$

⇒ Step 2.4: calculate new value of $v_{n+\frac{1}{2}}$:

$$v_{i,n+\frac{1}{2}} = v_{i,n+\frac{1}{2}} - \beta_n \frac{x_{i,n} - x_{j,n}}{m_i} \quad (4.15)$$

$$v_{j,n+\frac{1}{2}} = v_{j,n+\frac{1}{2}} + \beta_n \frac{x_{i,n} - x_{j,n}}{m_i} \quad (4.16)$$

⇒ Step 2.5: if all particles respect the tolerance or the upper iteration limit is reached, go on, otherwise return to Step 2.1

→ Step 3: calculate new particle coordinates using eq.4.2

→ Step 4: calculate new particle velocities at time step $n + 1$ using eq.4.3

→ Step 5: execute the velocity correction loop for all bonds in particle pairs:

⇒ Step 5.1: calculate inter-particle distance $\Gamma_{i,j}$, and if $|(v_{i,n+1} - v_{j,n+1})(x_{i,n+1} - x_{j,n+1})| <$

4| Langevin dynamics model

δ_v then go to Step 5.3, otherwise calculate the correction coefficient $\sigma_{i,j}$:

$$\sigma_{i,j} = \frac{(v_{i,n+1} - v_{j,n+1})(x_{i,n+1} - x_{j,n+1})}{d_{i,j}^2(\frac{1}{m_i} + \frac{1}{m_j})} \quad (4.17)$$

⇒ Step 5.2: calculate new $n + 1$ velocities as:

$$v_{i,n+1} = v_{i,n+1} - \sigma_{i,j,n+1} \frac{x_{i,n+1} - x_{j,n+1}}{m_i} \quad (4.18)$$

$$v_{j,n+1} = v_{j,n+1} + \sigma_{i,j,n+1} \frac{x_{i,n+1} - x_{j,n+1}}{m_i} \quad (4.19)$$

⇒ Step 5.3: if relative particle displacements in all particles are within some tolerances or the upper iteration limit is reached, go on, otherwise return to Step 5.1.

→ Step 6: if the actual time step is the last one then the algorithm is finished, otherwise return to Step 1.

4.2. Simulation details

	oil	silica	magnetite
ρ [Kg/m ³]	870	2650	5170
A [J]	$3.9 \cdot 10^{-21}$	$4.6 \cdot 10^{-21}$	$5.52 \cdot 10^{-19}$
ζ [mV]	-10	35	-33

Table 4.1: Particle Features: where A is the Hamaker constant, ρ is the density, and ζ is the zeta-potential.

Two oil droplets are generated in a simulation box, their respective diameters are 600 and 540nm, and their initial center-center distance is 800nm. During the time integration, silica and magnetite nano-particles are randomly generated, newly created sediment diameters are chosen randomly from a normal distribution centered in 30nm for silica and 70nm for magnetite. The generation position is randomized, with the constraint that the born particle surface distance from the existing particles has to be greater than 10nm, to prevent instabilities in the simulation.

Tolerances in the correction loops are set differently, as for the first one it is set as follows:

$$toll_{1-loop} = \sum_{i=1}^{n_{particles}} \sum_{j=1}^{n_{particles}} \frac{\Gamma_{i,j}}{n_{particles}^2 \omega} \quad (4.20)$$

4| Langevin dynamics model

where ω is an arbitrary coefficient, n is the particle counter index and Γ is the center-center distance; for the second loop, instead, the tolerance is fixed during the whole simulation as 10^{-10} .

Since the energy of desorption is much higher than the energy due to the Brownian motion and Van der Waals forces, particle-droplet contact is considered irreversible, anyways the sediment can freely move on the surface of the oil bubble, this constraint is applied once every time-step as described here:

$$\mathbf{x}_{\text{sediment}}^{\text{new}} = \mathbf{x}_{\text{droplet}} + \mathbf{v}(\mathbf{x}_{\text{sediment}}^{\text{old}}) \cdot d_{\text{sediment,droplet}} \quad (4.21)$$

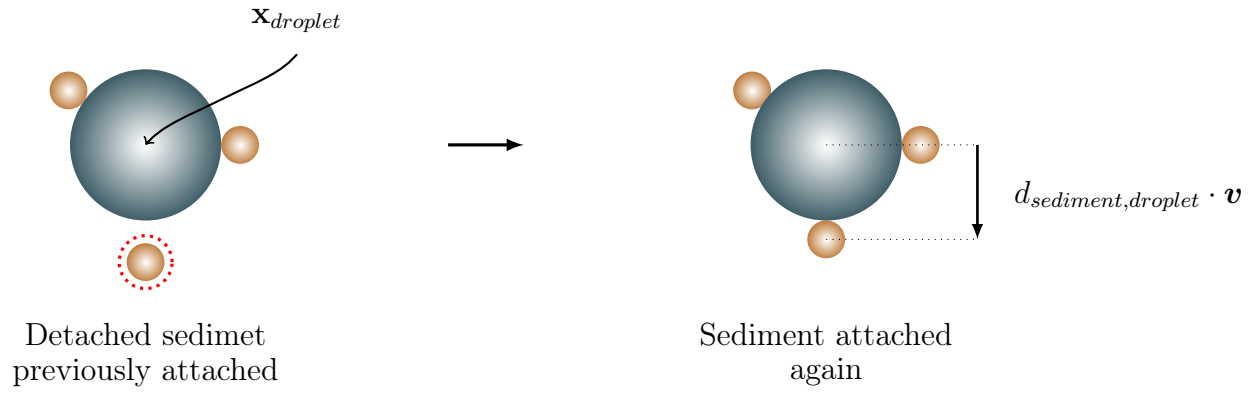


Figure 4.1: Representation of the snapping process.

where \mathbf{x} is the position vector and \mathbf{v} is the versor starting from the droplet center and pointing the particle center (fig.4.1). In order to increase the stability of the system the snapping procedure could be placed right after each corrector loop, but this would further increase the computational cost. The energy of detachment from the droplet varies from 40 to 2150kT for silica nano-particles, and from 840 to 46800kT for magnetite ones depending on the contact angle (30° to 90°); that is, the energy needed for the separation is much more than the thermal energy. Eq.4.22 is used to evaluate the said dis-joining energy, considering a typical value for alkane-water interface tension $\phi = 50mN/m$ (fig.4.2b).

$$E = \pi r^2 \phi (1 - \cos(\theta))^2 \quad (4.22)$$

The rest of the particle features are presented in tab.4.1, those values come from experimental

4| Langevin dynamics model

results at pH 8.

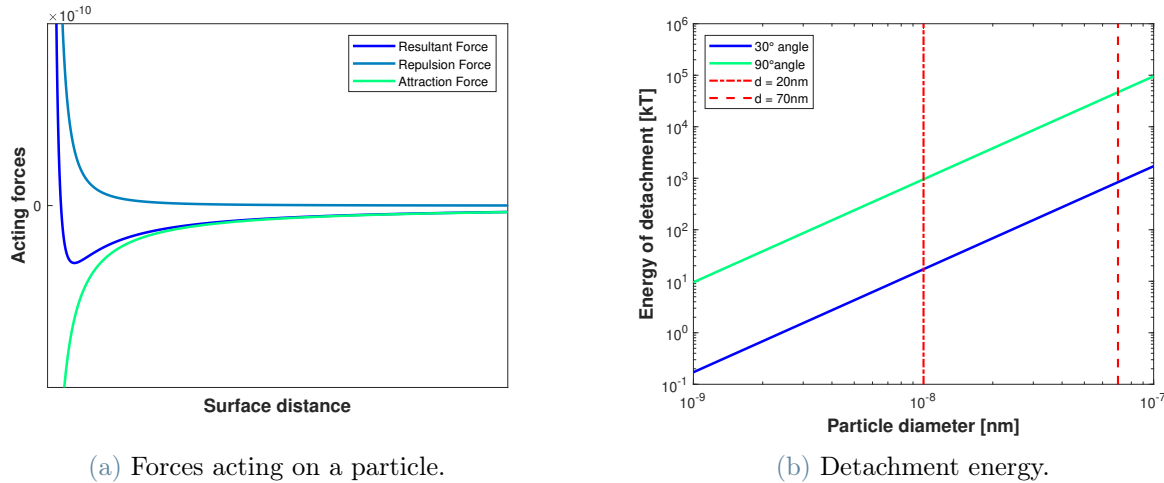


Figure 4.2

4.3. Results and conclusions

For the first micro-seconds sediments are adsorbed very slowly on the surface of the droplet, thus resulting in an almost constant surface distance, then, since the concentration of sediment is randomly increasing in time, forces acting on the droplets are becoming relevant, so they start moving towards each other up to a formation of a cluster. In the said cluster, sediments are not only attached to the surface of oil, but are also forming chain-like heteroaggregates, that grow up forming a more and more intricate structure as time passes. Fig.4.3a and 4.3b show two different time snapshots, respectively at $2 \cdot 10^{-6}\text{s}$ and $4.5 \cdot 10^{-6}\text{s}$, in the first one can't be recognised a formed inter-droplet structure, but only heteroaggregates floating around and a few adsorbed particles. In the second figure, instead, the number of attached sediments is much higher, and nano-particle-aggregates tend to arrange between oil, forming a stable emulsion. Fig.4.4a reveals that for the first $3.5 \cdot 10^{-6}\text{s}$ the inter-droplet distance remains essentially constant, although, in the next micro-seconds there is a sharp decrease in the mentioned variable, as if a critical sediments concentration has been reached.

4 | Langevin dynamics model

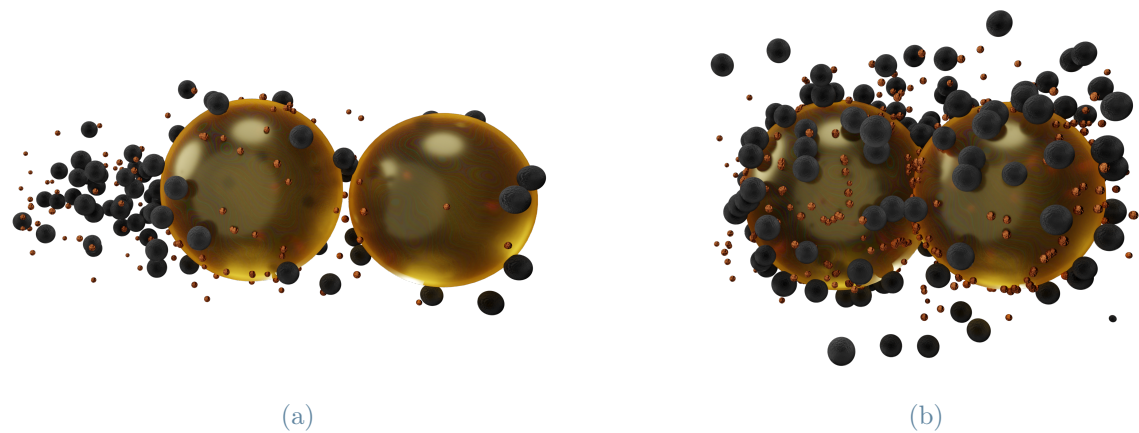


Figure 4.3: Snapshot of clusters at different times

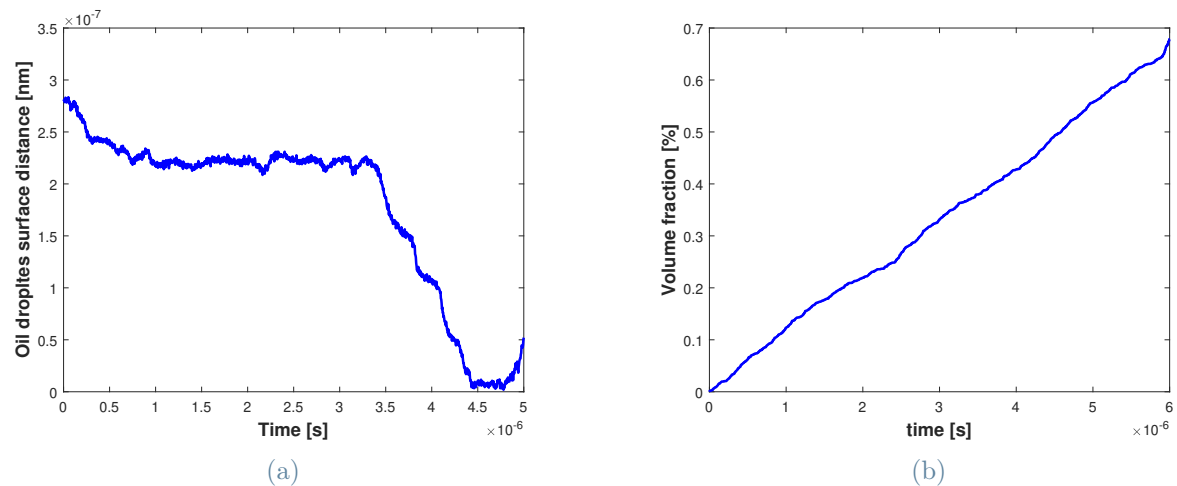


Figure 4.4: Oil droplet surface distance and sediments volume fraction varying in time.

Bibliography

- [1] H. C. Andersen. Rattle: A “velocity” version of the shake algorithm for molecular dynamics calculations. *Journal of Computational Physics*, 52(1):24–34, 1983. ISSN 0021-9991. doi: [https://doi.org/10.1016/0021-9991\(83\)90014-1](https://doi.org/10.1016/0021-9991(83)90014-1). URL <https://www.sciencedirect.com/science/article/pii/0021999183900141>.
- [2] G. Delvigne and C. Sweeney. Natural dispersion of oil. *Oil and Chemical Pollution*, 4(4):281–310, 1988. ISSN 0269-8579. doi: [https://doi.org/10.1016/S0269-8579\(88\)80003-0](https://doi.org/10.1016/S0269-8579(88)80003-0). URL <https://www.sciencedirect.com/science/article/pii/S0269857988800030>.
- [3] P. Hill, A. Khelifa, and K. Lee. Time scale for oil droplet stabilization by mineral particles in turbulent suspensions. *Spill Science Technology Bulletin*, 8(1):73–81, 2002. ISSN 1353-2561. doi: [https://doi.org/10.1016/S1353-2561\(03\)00008-2](https://doi.org/10.1016/S1353-2561(03)00008-2). URL <https://www.sciencedirect.com/science/article/pii/S1353256103000082>. Oil-Particle Interactions: Mechanisms, Environmental Significance, and Potential Applications.
- [4] M. Koroleva and E. Yurtov. Pickering emulsions stabilized with magnetite, gold, and silica nanoparticles: Mathematical modeling and experimental study. *Colloids and Surfaces A: Physicochemical and Engineering Aspects*, 601:125001, 2020. ISSN 0927-7757. doi: <https://doi.org/10.1016/j.colsurfa.2020.125001>. URL <https://www.sciencedirect.com/science/article/pii/S092777572030594X>.
- [5] MATLAB. 9.7.0.1190202 (r2022b). 2022. URL <https://it.mathworks.com>.
- [6] T. Nallamilli, E. Mani, and M. G. Basavaraj. A model for the prediction of droplet size in pickering emulsions stabilized by oppositely charged particles. *Langmuir*, 30(31):9336–9345, 2014. doi: [10.1021/la501785y](https://doi.org/10.1021/la501785y). URL <https://doi.org/10.1021/la501785y>. PMID: 25054284.
- [7] J. R. Payne, J. R. Clayton, and B. E. Kirstein. Oil/suspended particulate material interactions and sedimentation. *Spill Science Technology Bulletin*, 8(2):201–221, 2003. ISSN 1353-2561. doi: [https://doi.org/10.1016/S1353-2561\(03\)00048-3](https://doi.org/10.1016/S1353-2561(03)00048-3). URL <https://www.sciencedirect.com/science/article/pii/S1353256103000483>. Longer-Term Weathering Processes of Spilled Oil.

4| BIBLIOGRAPHY

- [8] P. G. Saffman and J. S. Turner. On the collision of drops in turbulent clouds. *Journal of Fluid Mechanics*, 1:16 – 30, 1956.
- [9] Y. Stern, R. Tadmor, V. Multanen, and G. Oren. A first order-based model for the kinetics of formation of pickering emulsions. *Journal of Colloid and Interface Science*, 628:409–416, 2022. ISSN 0021-9797. doi: <https://doi.org/10.1016/j.jcis.2022.07.110>. URL <https://www.sciencedirect.com/science/article/pii/S0021979722012917>.
- [10] Y. Yan and J. H. Masliyah. Effect of oil viscosity on the rheology of oil-in-water emulsions with added solids. *The Canadian Journal of Chemical Engineering*, 71(6):852–858, 1993. doi: <https://doi.org/10.1002/cjce.5450710605>. URL <https://onlinelibrary.wiley.com/doi/abs/10.1002/cjce.5450710605>.

List of Figures

1	Representation of different contact angles.	2
2	Oil spills in Mexican gulf, Cynthia.	3
1.1	Emulsification rate and number concentration of PE droplets as a function of time, with constant $\chi = 0.5$	7
1.2	Data fitting of the k parameter.	8
1.3	Formed Pickering emulsions in a oil-water system with sand as solid emulsifier. .	10
2.1	A_{obs} vs A_{theory} from Payne et al. (1989)	16
2.2	Distribution of OMA stabilization time lengths in time scale ranges	18
3.1	Variation of droplet diameter with composition.	22
3.2	Variation of $\frac{N_{eff}}{N_T}$ with composition.	23
3.3	Comparison between model and experimental data.	24
3.4	Effect of s on emulsion parameters.	25
4.1	Representation of the snapping process.	31
4.2	32
4.3	Snapshot of clusters at different times	33
4.4	Oil droplet surface distance and sediments volume fraction varying in time. . . .	33

List of Tables

1.1	Three different data sets for $\frac{N_{PE}}{N_{final}}$ with respect to time	9
2.1	Experimental data of Delvigne et al.(1987) and calculated values of α_{min}	14
2.2	Experimental data of Payne et al.(1989) and obtained values of α_{os}	15
2.3	Variables range to calculate OMA stabilization time	17
4.1	Particle Features: where A is the Hamaker constant, ρ is the density, and ζ is the zeta-potential.	30

